Quantitative comparison between Z(1/2) center and carbon vacancy in 4H-SiC

Koutarou Kawahara, Xuan Thang Trinh, Nguyen Tien Son, Erik Janzén, Jun Suda and Tsunenobu Kimoto

Original Publication:

Koutarou Kawahara, Xuan Thang Trinh, Nguyen Tien Son, Erik Janzén, Jun Suda and Tsunenobu Kimoto, Quantitative comparison between Z(1/2) center and carbon vacancy in 4H-SiC, 2014, Journal of Applied Physics, (115), 14, 143705.
http://dx.doi.org/10.1063/1.4871076

Quantitative comparison between Z12 center and carbon vacancy in 4H-SiC

Koutarou Kawahara, Xuan Thang Trinh, Nguyen Tien Son, Erik Janzén, Jun Suda, and Tsunenobu Kimoto

Citation: Journal of Applied Physics **115**, 143705 (2014); doi: 10.1063/1.4871076
View online: http://dx.doi.org/10.1063/1.4871076
View Table of Contents: http://scitation.aip.org/content/aip/journal/jap/115/14?ver=pdfcov
Published by the AIP Publishing

Quantitative comparison between $Z_{1/2}$ center and carbon vacancy in 4H-SiC

Koutarou Kawahara,[1,a)] Xuan Thang Trinh,[2] Nguyen Tien Son,[2] Erik Janzén,[2] Jun Suda,[1] and Tsunenobu Kimoto[1,b)]
[1]*Department of Electronic Science and Engineering, Kyoto University, Katsura, Nishikyo, Kyoto 615-8510, Japan*
[2]*Department of Physics, Chemistry and Biology, Linköping University, 581 83 Linköping, Sweden*

(Received 26 February 2014; accepted 31 March 2014; published online 9 April 2014)

In this study, to reveal the origin of the $Z_{1/2}$ center, a lifetime killer in n-type 4H-SiC, the concentrations of the $Z_{1/2}$ center and point defects are compared in the same samples, using deep level transient spectroscopy (DLTS) and electron paramagnetic resonance (EPR). The $Z_{1/2}$ concentration in the samples is varied by irradiation with 250 keV electrons with various fluences. The concentration of a single carbon vacancy (V_C) measured by EPR under light illumination can well be explained with the $Z_{1/2}$ concentration derived from *C-V* and DLTS irrespective of the doping concentration and the electron fluence, indicating that the $Z_{1/2}$ center originates from a single V_C. © *2014 AIP Publishing LLC*. [http://dx.doi.org/10.1063/1.4871076]

I. INTRODUCTION

SiC is a fascinating semiconductor that realizes high-power, high-temperature, and high-frequency devices. Because the $Z_{1/2}$ center[1–3] is a deep level known as a lifetime killer in n-type 4H-SiC,[4–6] identifying the origin of the $Z_{1/2}$ center is required for controlling carrier lifetimes in SiC.

The origin of the $Z_{1/2}$ center has been extensively investigated and suggested by different experimental studies to be a defect involving a carbon vacancy (V_C) because (i) this defect can be generated by electron irradiation with energies as low as 100 keV,[7–9] which corresponds to the energy threshold that can displace only carbon atoms in SiC, (ii) a lower $Z_{1/2}$ concentration is observed in SiC epilayers grown under C-rich condition,[10] (iii) the $Z_{1/2}$ center is a thermally stable defect[1] showing no changes in concentration up to 1600 °C,[8,11] indicating that the involvement of interstitials are unlikely, and (iv) the $Z_{1/2}$ center is efficiently eliminated by C^+ implantation followed by annealing.[12] The results from these electrical characterizations, however, can provide neither the microscopic model of $Z_{1/2}$ nor direct evidence proving that the defect is V_C-related. Recently, using *ab initio* calculation, it has been suggested that the $Z_{1/2}$ center originates from the double acceptor (2–/0) level of V_C.[13] Based on the correlation between the energy position in the bandgap of the $Z_{1/2}$ center determined by deep level transient spectroscopy (DLTS) and that of V_C by electron paramagnetic resonance (EPR), the $Z_{1/2}$ center was assigned to the (2–/0) level of V_C.[14] Furthermore, it has been shown that the $Z_{1/2}$ center and V_C defect are the dominant defects and are responsible for carrier compensation in electron irradiated SiC,[15] further supporting that the $Z_{1/2}$ center originates from V_C. Even by these continuous studies, however, a direct quantitative evidence showing the origin of the $Z_{1/2}$ center has not been achieved.

In this paper, we will show that the origin of the $Z_{1/2}$ center is a single V_C by investigating the correlation between the concentration of the $Z_{1/2}$ center obtained by capacitance-voltage (*C-V*) or DLTS and that of V_C by EPR in n-type 4H-SiC irradiated by low-energy (250 keV) electrons with various electron fluences. It is noted that the direct comparison of DLTS and EPR results is not easy due to the following three reasons. (i) EPR measurements are suitable for relatively high defect concentrations (over $\sim 10^{12}$ spins, which correspond to a concentration over $\sim 10^{15}\,cm^{-3}$ if samples are thin films). For DLTS measurements, however, a low trap concentration N_T as compared to the donor concentration N_d ($N_T < 0.2N_d$) is required (typical N_d in SiC epilayers employed for this kind of study has been 10^{14}–$10^{16}\,cm^{-3}$). (ii) By DLTS, only regions near the surface are monitored (a trap volume density near the surface is obtained), whereas EPR has no spatial resolution (EPR signal results from the center distributing in the whole sample and thereby an area density of a defect is obtained). To compare a trap volume density measured by DLTS with an area density of a defect by EPR, a depth profile of the trap volume density has to be known. (iii) The detectable defects by EPR depend on the charge state of the defects; for V_C, V_C^- is detectable, whereas V_C^{2-} and V_C^0 are EPR-inactive. Because the V_C defect has a negative-U nature,[13,14,16] in n-type material most V_C defects are either in the neutral or 2– charge states under equilibrium condition and, hence, cannot be detected by EPR. Due to the restriction (i), in a previous study,[17] electron fluences used for samples measured by DLTS were much lower than those used for samples studied by EPR, which prevented a direct comparison in concentration between the $Z_{1/2}$ deep level and the C vacancy.

In this study, we overcame the restrictions (i)–(iii) by the following solutions (i)–(iii), respectively. (i) n-type 4H-SiC epilayers with relatively high doping concentrations (10^{16}–$10^{18}\,cm^{-3}$) were irradiated by low-energy (250 keV) electrons with various electron fluences, introducing various concentrations of the $Z_{1/2}$ center. On these samples, DLTS and EPR measurements could be performed, allowing a direct

a)Electronic mail: kawahara@semicon.kuee.kyoto-u.ac.jp
b)Also at Photonics and Electronics Science and Engineering Center (PESEC), Kyoto University, Kyoto, Japan.

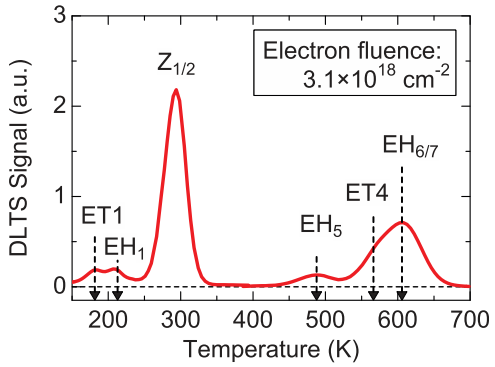

FIG. 1. DLTS spectra observed in a D sample (N_d : 1.6×10^{17} cm^{-3}) irradiated with an electron fluence of 3.1×10^{18} cm^{-2}.

comparison of the results obtained from the two techniques. (ii) Because the $Z_{1/2}$ center is not uniformly distributed along the depth in the irradiated samples (as described in Sec. III B), we measured the $Z_{1/2}$ concentration by repeating DLTS measurements and mechanical polishing many times, and integrated the volume concentrations over the entire depth (resulting in the trap area density, which can be compared with an area density of a defect measured by EPR). In addition, for EPR measurements, we used 100 μm-thick epilayers after removal of the substrates by mechanical polishing. (iii) By light excitation, V_C^- can be activated and measured by EPR. The ratio of the V_C concentration in each charge state was consistently taken into account for comparison in concentration between $Z_{1/2}$ and V_C.

II. EXPERIMENTS

The starting materials are 100 μm-thick n-type 4H-SiC epilayers. The doping concentration N_d is varied by wafers: (A) 1.8×10^{16} cm^{-3}, (B) 3.8×10^{16} cm^{-3}, (C) 1.1×10^{17} cm^{-3}, (D) 1.6×10^{17} cm^{-3}, and (E) 1.2×10^{18} cm^{-3}. The epilayers were irradiated by 250 keV electrons with different fluences of 1×10^{15}–1×10^{19} cm^{-2}. Ni/SiC Schottky structures were formed on the samples used for *C-V*, *I–V*, and DLTS measurements, while the substrates of the other set of samples used for EPR measurements were removed by mechanical polishing. For data sampling in all DLTS measurements, a period width of 0.205 s and a probe frequency of 1 MHz were employed. In DLTS measurements, the reverse bias voltage was varied in the range from 0 V to –100 V, which corresponds to monitored depths of about 0.1–1.4 μm in samples of the wafer B (named B samples). EPR measurements were performed on an X-band (~9.4 GHz) Bruker E500 spectrometer equipped with a continuous He-flow cryostat, allowing the sample temperature regulation in the range of 4–295 K. In photoexcitation EPR (photo-EPR) experiments, a 200 W halogen lamp and appropriate optical filters were used for excitation.

III. RESULTS

A. Deep levels in electron-irradiated samples

Figure 1 shows DLTS spectra observed in a D sample (N_d: 1.6×10^{17} cm^{-3}) irradiated with an electron fluence of 3.1×10^{18} cm^{-2}. In this sample, the ET1 ($E_C - 0.30$ eV),[8] EH_1 ($E_C - 0.34$ eV),[18] $Z_{1/2}$ ($E_C - 0.67$ eV),[1] EH_5 ($E_C - 1.3$ eV),[18] ET4 ($E_C - 1.3$ eV), and $EH_{6/7}$ ($E_C - 1.5$ eV)[18] centers were observed. The activation energy was derived by assuming a temperature-independent capture cross section. Taking into account temperature dependence of the capture cross section of the $Z_{1/2}$ level (the activation energy: 0.074 eV (Refs. 19 and 20)), the energy level of the $Z_{1/2}$ center is recalculated as $E_C - 0.59$ eV. All these deep levels are often observed in irradiated 4H-SiC except for the ET4 center, which is not easy to be separated from the $EH_{6/7}$ center because of severe overlapping. Among these centers, the $Z_{1/2}$ center showed the highest concentration in the irradiated samples.

B. Depth profiles of $Z_{1/2}$ center after electron irradiation

By DLTS and *C-V* measurements, the $Z_{1/2}$ concentration in the irradiated samples was investigated. Note that after electron irradiation the $Z_{1/2}$ center does not uniformly distribute along the depth of the epilayers. Figure 2(a) shows depth profiles of the $Z_{1/2}$ center in lightly doped epilayers (N_d: 1.6×10^{15} cm^{-3}, initial $Z_{1/2}$ concentration: 1.7×10^{13} cm^{-3}) after irradiation with 250 keV electrons with relatively low fluences (3×10^{15}–2×10^{16} cm^{-2}). The distribution of the $Z_{1/2}$ center can be roughly fitted by the following equation:

$$N_T(x) = N_0 + N_{surf} \exp(-3.8 \times 10^4 x^2), \quad (1)$$

where x signifies the distance from the surface (cm), N_{surf} the $Z_{1/2}$ concentration at the surface, and N_0 the initial $Z_{1/2}$ concentration before electron irradiation. The N_{surf} values in the irradiated samples are easily measured by DLTS. Figure 2(b) shows the dependence of N_{surf} on irradiated electron fluence

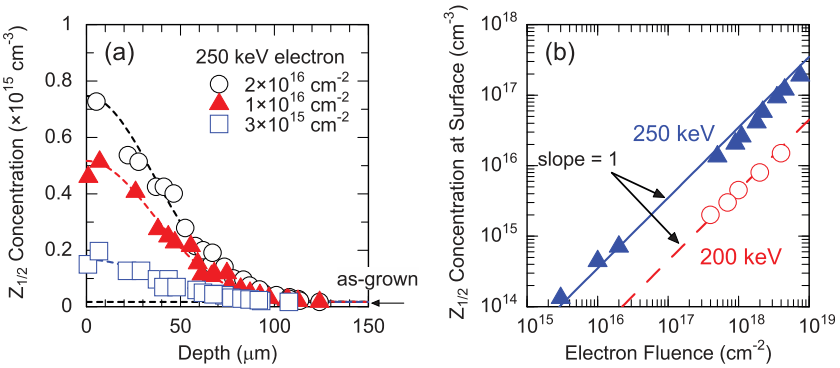

FIG. 2. (a) Depth profiles of the $Z_{1/2}$ center in lightly doped 4H-SiC epilayers (N_d: 1.6×10^{15} cm^{-3}, initial $Z_{1/2}$ concentration: 1.7×10^{13} cm^{-3}) after irradiation with 250 keV electrons with various fluences (circles: 2×10^{16} cm^{-2}, triangles: 1×10^{16} cm^{-2}, and squares: 3×10^{15} cm^{-2}). Each dashed line indicates a fitting curve following Eq. (1). (b) Dependence of the $Z_{1/2}$ concentration near the surface region measured by DLTS on the irradiated electron fluence (electron energy: 200 keV or 250 keV).

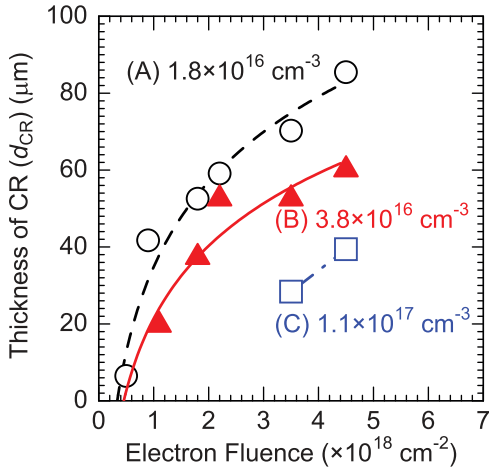

FIG. 3. Dependence of the CR thickness (d_{CR}) in the A–C samples (circles: A samples, triangles: B samples, and squares: C samples) derived from *C-V* results on the irradiated electron fluence.

(electron energy: 200 keV or 250 keV), which is in proportion to the electron fluence in the wide range. The proportional coefficients between the $Z_{1/2}$ concentration and electron fluence are $4.5 \times 10^{-2}\,cm^{-1}$ for 200 keV electrons and $3.5 \times 10^{-2}\,cm^{-1}$ for 250 keV electrons, which does not conflict with a previous report[9] (the slight difference may be due to a difference of the monitored depth).

The depth profiles of $Z_{1/2}$ center can also be estimated by the thickness of a compensated region (CR). When the electron fluence is very high, a semi-insulating region was formed due to compensation, which resulted in an almost bias-independent capacitance in *C-V* measurements. The CR is formed where the $Z_{1/2}$ concentration exceeds N_d and the deep center can capture almost all electrons from the N shallow donors. Figure 3 shows the dependence of the CR thickness (d_{CR}) on the electron fluence, which was derived from the equation: $d_{CR} = \epsilon/C$ (ϵ: dielectric constant, C: capacitance per unit area obtained from *C-V* measurements). Because the CR region is formed where the trap concentration exceeds the doping concentration, electron irradiation with higher fluence or lower doping concentration leads to thicker d_{CR}. When $N_T(d_{CR}) = N_d$ is applied to Eq. (1), the N_{surf} value in each sample can be obtained from each d_{CR} (derived from *C-V* results). Figure 4 shows the N_{surf} values of A–C samples obtained from DLTS measurements and from *C-V* measurements. The plots from *C-V* measurements are roughly on a line independent of the donor concentration, suggesting that the depth profiles of the $Z_{1/2}$ center estimated from *C-V* results are valid. The slight difference between the DLTS results and the *C-V* results may be attributed to the overestimation of N_{surf} values in Eq. (1). In this study, the $Z_{1/2}$ depth profiles derived from *C-V* results (profiles obtained from d_{CR} determined by the points where $N_T = N_d$) are employed for the comparison in concentration between $Z_{1/2}$ and V_C.

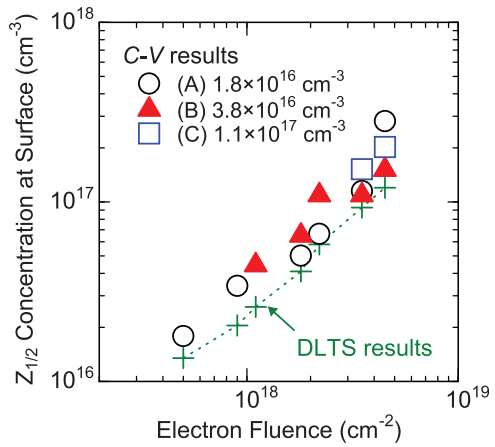

FIG. 4. $Z_{1/2}$ concentration near the surface (N_{surf}) of the A–C samples obtained from DLTS measurements and *C-V* results with Eq. (1).

C. Charge states of V_C in darkness and under illumination

In the bandgap of 4H-SiC, V_C can be in several charge states such as V_C^{2-}, V_C^-, V_C^0, V_C^+, or V_C^{2+} (Refs. 13, and 21–23), among which V_C^{2-}, V_C^-, and V_C^0 are expected to be present in n-type materials. Because V_C^{2-} and V_C^0 have the electron spin $S = 0$ and cannot be detected by EPR, the V_C^- concentration in the irradiated samples was investigated. Figure 5 shows EPR spectra for a C sample irradiated with a fluence of $4.5 \times 10^{18}\,cm^{-2}$ measured at 100 K in darkness or under illumination with light of photon energies ≃1.6 eV. In all samples having a CR, two signals, showing g values ($\boldsymbol{B} \parallel \boldsymbol{c}$) of 2.00475 and 2.00398, were dominant. From the obtained g tensor and the Si hyperfine (hf) tensors, the spectra were identified to be V_C^- signals at the cubic site ($V_C^-(k)$) and at the hexagonal site ($V_C^-(h)$).[14,24] Under illumination, the $V_C^-(h)$ signal clearly increased and the $V_C^-(k)$ signal appeared, which can be explained by negative-U nature of V_C.[13,14] In equilibrium for n-type SiC, V_C^- prefers capturing another electron to relax to the lower-lying 2– state which is EPR inactive. Illumination excites an electron from the 2– state to the conduction band, activating the single negative charge state and, hence, leading to the appearance and increase of the V_C^- signal.

Figure 6 shows the schematic diagram for the electron transitions between the V_C levels ($V_C^{2-/0}$ level (When the Fermi level is located above/below this level, V_C^{2-}/V_C^0 is energetically favorable. However, note that this level corresponds to the V_C transitions between V_C^{2-} and V_C^-.) and $V_C^{-/0}$ level) and the conduction band E_C. The ratio of the V_C

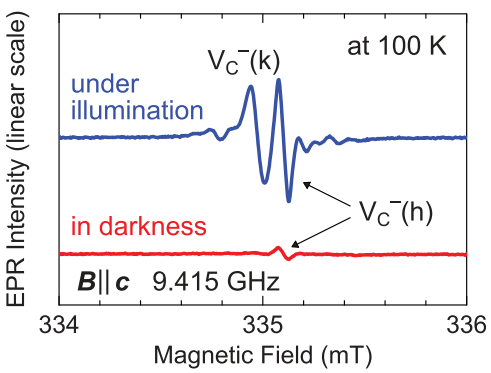

FIG. 5. EPR spectra for the C sample irradiated with a fluence of $4.5 \times 10^{18}\,cm^{-2}$ measured at 100 K in darkness or under illumination with light of photon energies ≃1.6 eV.

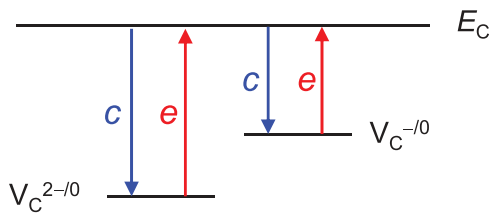

FIG. 6. Schematic diagram for the electron transitions between the V_C levels ($V_C^{2-/0}$ and $V_C^{-/0}$) and the conduction band.

concentration in each charge state ($[V_C^{2-}] : [V_C^{-}] : [V_C^{0}]$) should be determined by the electron capture (c) and emission (e) rate

$$c = \sigma v_{th} n, \tag{2}$$

$$e = \sigma v_{th} N_C \exp\left(-\frac{E_C - E_T}{kT}\right) + \alpha A(\Delta E_{light}), \tag{3}$$

where σ denotes the electron capture cross section, v_{th} the thermal velocity of electrons, n the carrier concentration (electrons in the conduction band), α the probability of the electron being excited by photons. In Eq. (3), the first term corresponds to thermal emission of electrons from a trap located at E_T to the conduction band edge, whereas the second term corresponds to electron emission by photoexcitation. A is a function of $\Delta E_{light} = E_{light} - (E_C - E_T + E_{FC})$ ($A = 0$ when $\Delta E_{light} \leq 0$), where E_{FC} signifies the Franck-Condon shift and E_{light} the photon energy. When the occupancy ratio of a trap is given as f, the relation of f, c, and e in the steady state is described as

$$\frac{f}{1-f} = \frac{c}{e}. \tag{4}$$

When Eqs. (2)–(4) are applied for all traps located in the bandgap of the samples (e.g., $V_C^{2-/0}$(h), $V_C^{2-/0}$(k), $V_C^{-/0}$(h), $V_C^{-/0}$(k)), the accurate occupancy ratio of the traps can be achieved. Even without solving all the equations, most behaviors of V_C^- signals during EPR measurements can qualitatively be explained as follows. No V_C^- signals could be observed in heavily doped E samples ($N_d = 1.2 \times 10^{18}\,cm^{-3}$). In the region where the doping concentration exceeds the trap concentration, the carrier concentration n is much higher than that in CR. Therefore, the electron capture rate c was high (from Eq. (2)), and there are enough carriers to transform almost all V_C to V_C^{2-}. In other words, when there exists a high density of electrons in the conduction band, V_C immediately captures electrons and becomes V_C^{2-} even under illumination. In CR, in contrast, a large part of the total concentration of V_C can be in the negative charge state V_C^- under illumination because electron capture rate of V_C^- is small.

D. Concentration comparison between $Z_{1/2}$ and V_C

In this section, the V_C^- area density $[V_C^-]_A$ measured by EPR in the A–C samples irradiated with various electron fluences is compared with the "maximum $Z_{1/2}^-$ area density $[Z_{1/2}^-]_{MAX}$" derived from DLTS and *C-V* results. As mentioned in Sec. III B, the depth profiles of the $Z_{1/2}$ center can be estimated from the DLTS and *C-V* results. Using the depth profile of the $Z_{1/2}$ center, $[Z_{1/2}^-]_{MAX}$ can be estimated as the area shown as "$[Z_{1/2}^-]_{MAX}$" in Fig. 7. Figure 7 shows the schematic diagram of the depth profiles of the $Z_{1/2}$ concentration obtained by DLTS ($[Z_{1/2}]_{DLTS}$) and the real concentration of the $Z_{1/2}$ center ($[Z_{1/2}]$) in the sample irradiated with a high electron fluence. Here, note that the $Z_{1/2}$ concentration measured by DLTS is twice higher than the real $Z_{1/2}$ concentration because the $Z_{1/2}$ center captures two electrons. The thickness of a CR (d_{CR}) can be defined by the depth at the cross point of the donor concentration N_d and $[Z_{1/2}]_{DLTS}$. Almost all V_C located out of CR should be V_C^{2-} because in this region a high density of electrons exists in the conduction band, leading to the high electron-capture rate of V_C (from Eq. (2)). Within the CR, in contrast, $[Z_{1/2}^-]$ is limited by $[Z_{1/2}]$ and N_d because an electron is needed for $Z_{1/2}$ to become $Z_{1/2}^-$.

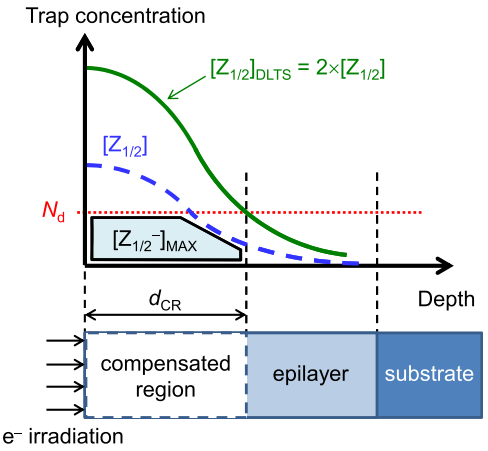

FIG. 7. Schematic diagram of the depth profiles of the $Z_{1/2}$ center obtained by DLTS ($[Z_{1/2}]_{DLTS}$) and real $Z_{1/2}$ center ($[Z_{1/2}]$) in the sample irradiated with a high electron fluence. The area shown as "$[Z_{1/2}^-]_{MAX}$" denotes the maximum $Z_{1/2}^-$ area density.

Figure 8(a) shows $[V_C^-]_A$ as a function of the electron fluence in the A–C samples measured by EPR under illumination with light of photon energies $\simeq$1.6 eV. Higher electron fluence leads to higher $[V_C^-]_A$. Fig. 8(b) shows $[V_C^-]_A$ measured by EPR as a function of $[Z_{1/2}^-]_{MAX}$ estimated from DLTS and *C-V* results (determined from the depth profiles of the $Z_{1/2}$ center). All the plotted data show $[V_C^-]_A \simeq [Z_{1/2}^-]_{MAX}$ irrespective of the doping concentration and the electron fluence, indicating that the V_C and $Z_{1/2}$ volume densities have a one-to-one correspondence. Here, $[V_C^-]_A$ is 30%–40% lower than $[Z_{1/2}^-]_{MAX}$ because not all V_C is in the single-negative charge state even under illumination due to a high electron-capture rate of V_C^-. The charge states of the V_C defects are further discussed in Sec. IV. From this quantitative correlation in concentration, it is strongly suggested that the origin of the $Z_{1/2}$ center is the single V_C.

IV. DISCUSSION

The ratio of $[V_C]$ in each charge state ($[V_C^{2-}] : [V_C^-] : [V_C^0]$) is further discussed because it is a key point of the concentration comparison between $Z_{1/2}$ and V_C. We focused on the three particular behaviors of the V_C^- signals for the A–C samples.

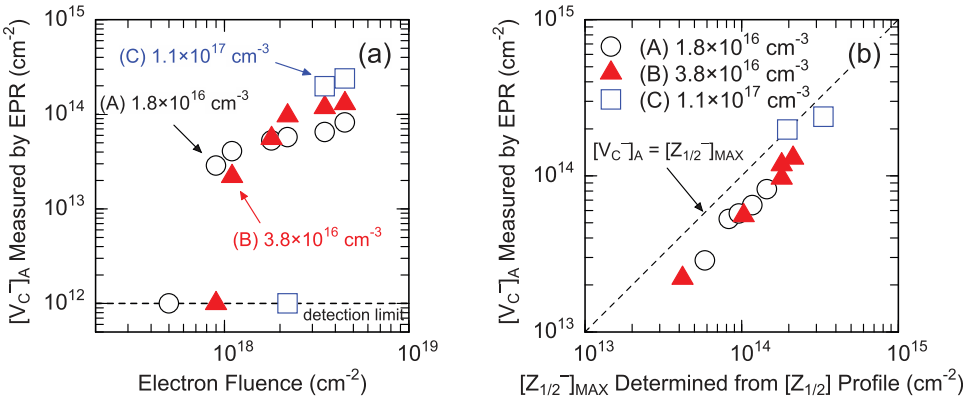

FIG. 8. (a) V_C^- area density $[V_C^-]_A$ as a function of the electron fluence in the A–C samples. (b) $[V_C^-]_A$ as a function of $[Z_{1/2}^-]_{MAX}$. $[V_C^-]_A$ was measured by photo-EPR, whereas $[Z_{1/2}^-]_{MAX}$ was estimated from the depth profiles of the $Z_{1/2}$ volume density obtained by DLTS and *C-V* measurements.

(i) The carrier concentration (the electron concentration in the conduction band) in CR is very low even under illumination. This is shown from EPR measurements of the A–C samples performed either in darkness or under illumination with high values of the quality factor Q, which are only attainable in samples having very low conductivity. In addition, at temperatures lower than 200 K, the V_C^- signal intensity was almost unchanged after turning off the light. This indicates that (a) there were few electrons in the conduction band even under illumination due to large cross section for capturing an electron to the neutral charge state and the higher concentration of V_C compared to that of the carrier concentration, and (b) few electrons were captured to the negative charge state after turning off the light due to the energy barrier for the transition. In fact, the $Z_{1/2}$ center has a large capture cross section for $Z_{1/2}^{-/0}$ (over $1 \times 10^{-14}\,cm^2$ compared to $-20 \times 10^{-19}\,cm^2$ for $Z_{1/2}^{2-/0}$ at 100 K) with an energy barrier for the transition "$Z_{1/2}^-$ to $Z_{1/2}^{2-}$" of 0.065–0.080 eV.[19,20]

(ii) The electron excitation probability by photons α (Eq. (3)) was nearly unity under the illumination condition (there exist sufficient photons to interact with electrons). The intensity of the V_C^- signal was almost constant when the power of excitation light was changed in the range over an order of magnitude, indicating that the excitation probability was saturated.

(iii) The electron emission rate by light excitation is much higher than that by thermal excitation (the first term of Eq. (3) is negligible) under the illumination at 100–200 K. Figure 9 shows the temperature dependence of $[V_C]_A$ in the A sample irradiated with a fluence of $4.5 \times 10^{18}\,cm^{-2}$ in darkness and under illumination. By light excitation, $[V_C^-]_A$ increased by about two orders of magnitude and did not depend on the measurement temperature, suggesting that thermal excitation of electrons is negligible under illumination. $[V_C^-]_V$ in darkness can be estimated using the equations

$$f_{(-/0)} = \frac{[V_C^-]}{[V_C^0] + [V_C^-]} = \frac{1}{1 + \exp\left(\frac{E_{T(-/0)} - E_F}{kT}\right)}, \quad (5)$$

$$f_{(2-/0)} = \frac{[V_C^{2-}]}{[V_C^-] + [V_C^{2-}]} = \frac{1}{1 + \exp\left(\frac{E_{T(2-/0)} - E_F}{kT}\right)}, \quad (6)$$

under the binding condition, $[V_C] = [V_C^{2-}] + [V_C^-] + [V_C^0]$ and $N_d = n + 2[V_C^{2-}] + [V_C^-]$, where $E_{T(-/0)}$ and $E_{T(2-/0)}$ signify the energy levels of $V_C^{-/0}$ and $V_C^{2-/0}$, respectively. Equations (5) and (6) suggest that the occupancy ratio of traps in darkness can be described by the Fermi-Dirac distribution function. As parameters, $E_C - E_{T(-/0)}$ and $E_C - E_{T(2-/0)}$ of 0.52 and 0.72 eV for h-site, 0.45 and 0.76 eV for k-site,[19] N_d of $1.8 \times 10^{16}\,cm^{-3}$, and $[V_C]_V$ of $3 \times 10^{16}\,cm^{-3}$ were assumed, where $[V_C]_V$ does not influence on the calculated results very much if the value sufficiently exceeds the half of N_d. The calculated $[V_C^-]_A (= [V_C^-] \cdot d_{CR})$ is shown in Fig. 9 as a dashed line ($[V_C^-(h)]_A$) and a solid line ($[V_C^-(k)]_A$). The calculated $[V_C^-]_A$ depends on the sites (h or k) and increases with the temperature due to the temperature dependence of the Fermi-Dirac distribution function. $[V_C^-(h)]_A$ and $[V_C^-(k)]_A$ were individually calculated for simplicity (all levels have to be solved together for an accurate calculation). At low temperatures (~100 K), the experimental $[V_C^-]_A$ in darkness is close to the calculated $[V_C^-(h)]_A$, whereas the $V_C^-(k)$ signal can hardly be detected and the calculated $[V_C^-(k)]_A$ is small. This is expected since the energy distance between the (2–/0) and (–/0) level of

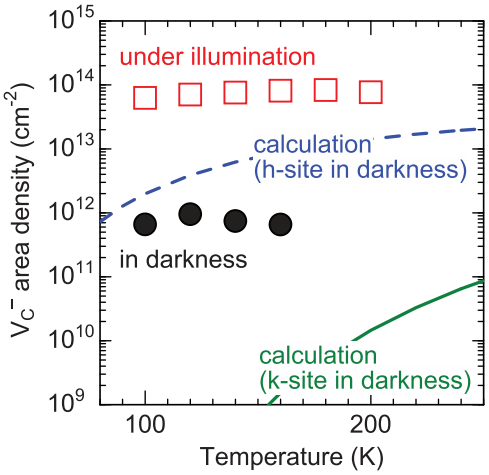

FIG. 9. Temperature dependence of V_C^- area density $[V_C^-]_A$ in the A sample irradiated with the fluence of $4.5 \times 10^{18}\,cm^{-2}$ in darkness (circles) and under illumination (squares). The lines indicate $[V_C^-]_A$ for h- or k-site in darkness (under equilibrium condition) estimated using Eqs. (5) and (6).

V_C is smaller for the h-site ($\sim 0.72–0.52 = 0.2$ eV) and larger for the k-site ($\sim 0.76–0.45 = 0.31$ eV). In darkness, the population of V_C^-, which is determined by thermal distribution between the (2–/0) and (–/0) levels, should be small at low temperatures in particular for the k-site. Thus, the concentration measured in darkness at low temperatures is close to the $[V_C^-(h)]_A$, which is a small part of the total concentration of V_C (mainly in the 2– charge state).

V. CONCLUSION

The concentration of the V_C defect in n-type 4H-SiC epilayers irradiated with 250 keV electrons measured by EPR was quantitatively compared with that of the $Z_{1/2}$ center measured by *C-V* and DLTS in the same sample sets. The $Z_{1/2}$ center and V_C defect are the dominant defects responsible for the carrier compensation observed in the irradiated samples. After the electron irradiation, the $Z_{1/2}$ center did not uniformly distribute along the depth, which could be reproduced by an equation with a parameter: the $Z_{1/2}$ concentration near the surface N_{surf} or the compensated region thickness d_{CR}. The $Z_{1/2}$ depth profiles estimated from the N_{surf} measured by DLTS agreed with those from the d_{CR} measured by *C-V* irrespective of the doping concentration and the electron fluence. With the depth profiles of the $Z_{1/2}$ center, maximum $Z_{1/2}^-$ area densities $[Z_{1/2}^-]_{MAX}$ were estimated and compared with the V_C^- area densities $[V_C^-]_A$ measured by EPR. $[Z_{1/2}^-]_{MAX}$ estimated from DLTS and *C-V* agrees well with $[V_C^-]_A$ measured by EPR irrespective of the doping concentration and the electron fluence (in 13 samples). Based on this direct quantitative comparison, it is concluded that the $Z_{1/2}$ center is related to the (2–/0) level of the single C vacancy.

ACKNOWLEDGMENTS

Support by the Grant-in-Aid for Scientific Research (21226008 and 80225078) from the Japan Society for the Promotion of Science, the Swedish Foundation for Strategic Research, the Swedish Research Council VR/Linné LiLi-NFM, and the Knut and Alice Wallenberg Foundation is gratefully acknowledged.

[1]T. Dalibor, G. Pensl, H. Matsunami, T. Kimoto, W. J. Choyke, A. Schöner, and N. Nordell, Phys. Status Solidi A **162**, 199 (1997).
[2]M. Weidner, T. Frank, G. Pensl, A. Kawasuso, H. Itoh, and R. Krause-Rehberg, Physica B **308–310**, 633 (2001).
[3]M. L. David, G. Alfieri, E. M. Monakhov, A. Hallén, C. Blanchard, B. G. Svensson, and J. F. Barbot, J. Appl. Phys. **95**, 4728 (2004).
[4]P. B. Klein, B. V. Shanabrook, S. W. Huh, A. Y. Polyakov, M. Skowronski, J. J. Sumakeris, and M. J. O'Loughlin, Appl. Phys. Lett. **88**, 052110 (2006).
[5]K. Danno, D. Nakamura, and T. Kimoto, Appl. Phys. Lett. **90**, 202109 (2007).
[6]P. B. Klein, J. Appl. Phys. **103**, 033702 (2008).
[7]L. Storasta, J. P. Bergman, E. Janzén, A. Henry, and J. Lu, J. Appl. Phys. **96**, 4909 (2004).
[8]K. Danno and T. Kimoto, J. Appl. Phys. **100**, 113728 (2006).
[9]H. Kaneko and T. Kimoto, Appl. Phys. Lett. **98**, 262106 (2011).
[10]T. Kimoto, S. Nakazawa, K. Hashimoto, and H. Matsunami, Appl. Phys. Lett. **79**, 2761 (2001).
[11]G. Alfieri, E. V. Monakhov, B. G. Svensson, and M. K. Linnarsson, J. Appl. Phys. **98**, 043518 (2005).
[12]L. Storasta and H. Tsuchida, Appl. Phys. Lett. **90**, 062116 (2007).
[13]T. Hornos, A. Gali, and B. G. Svensson, Mater. Sci. Forum **679–680**, 261 (2011).
[14]N. T. Son, X. T. Trinh, L. S. Løvlie, B. G. Svensson, K. Kawahara, J. Suda, T. Kimoto, T. Umeda, J. Isoya, T. Makino, T. Ohshima, and E. Janzén, Phys. Rev. Lett. **109**, 187603 (2012).
[15]K. Kawahara, X. T. Trinh, N. T. Son, E. Janzén, J. Suda, and T. Kimoto, Appl. Phys. Lett. **102**, 112106 (2013).
[16]X. T. Trinh, K. Szász, T. Hornos, K. Kawahara, J. Suda, T. Kimoto, A. Gali, E. Janzén, and N. T. Son, Phys. Rev. B **88**, 235209 (2013).
[17]P. Carlsson, N. T. Son, F. C. Beyer, H. Pedersen, J. Isoya, N. Morishita, T. Ohshima, and E. Janzén, Phys. Status Solidi RRL **3**, 121 (2009).
[18]C. Hemmingsson, N. T. Son, O. Kordina, J. P. Bergman, E. Janzén, J. L. Lindström, S. Savage, and N. Nordell, J. Appl. Phys. **81**, 6155 (1997).
[19]C. G. Hemmingsson, N. T. Son, A. Ellison, J. Zhang, and E. Janzén, Phys. Rev. B **58**, R10119 (1998); **59**, 7768 (1999).
[20]T. Kimoto, T. Yamamoto, Z. Y. Chen, H. Yano, and H. Matsunami, J. Appl. Phys. **89**, 6105 (2001).
[21]A. Zywietz, J. Furthmüller, and F. Bechstedt, Phys. Rev. B **59**, 15166 (1999).
[22]L. Torpo, M. Marlo, T. E. M. Staab, and R. M. Nieminen, J. Phys.: Condens. Matter **13**, 6203 (2001).
[23]M. Bockstedte, A. Mattausch, and O. Pankratov, Phys. Rev. B **69**, 235202 (2004).
[24]T. Umeda, Y. Ishitsuka, J. Isoya, N. T. Son, E. Janzén, N. Morishita, T. Ohshima, H. Itoh, and A. Gali, Phys. Rev. B **71**, 193202 (2005).